Strong electron–phonon interaction establishes correlation between superconducting and charge density wave states in NbSe$_2$

I. Naik* and S. Sethy

Department of Physics, North Orissa University,
Baripada 757 003, India

Here an analytical expression is proposed for the correlation between superconducting (SC) transition temperature (T_{sc}) derived by Louie and Cohen and charge density wave (CDW) transition temperature derived by Peierls at strong electron–phonon interaction. This expression was verified by the pressure effect T_{sc} and T_{cdw} of 2H-NbSe$_2$ with $m \approx 64.86$ and $c \approx 2.24$ as best-fitting parameters. From these parameters, phonon energies $\hbar\sqrt{\langle\omega_{sc}^2\rangle} \approx 3.8$ meV and $\hbar\omega_{cdw} \approx 1.4$ meV were calculated for SC and CDW states respectively. It also provides T_{cdw} very close to the experimental values of 2H- and 4H-NbSe$_2$, regardless of their stacking order and coordination difference.

Keywords: Charge density wave, phonon energy, superconductivity, transition-metal compound.

NbSe$_2$ is one of the group-V transition metal dichalcogenide compounds with chemical formula MX$_2$, where M is the transition metal atom and X is S, Se and Te, in which Nb atoms are sandwiched between two Se layers. In group-V transition metal dichalcogenides, the possible polymorphic phase transitions can be obtained by sintering the compounds at different temperatures[1]. Two polytypes of NbSe$_2$, 2H with trigonal prismatic coordination and 4H with alternatively octahedral and prismatic coordination of Nb atom have been reported, showing a charge density wave (CDW) followed by a superconducting (SC) transition at low temperature[2,3]. Though the mechanism of these two transitions is similar, due to electron–phonon (e–ph) interaction, the origin of CDW is not clearly understood till today because evidence of the CDW transition temperature T_{cdw} was reported on 2H-NbSe$_2$ using several methods[4–9]. Besides, T_{cdw} was found to be sensitive to crystal imperfection which does not affect the superconducting transition temperature T_{sc} in 2H-NbSe$_2$ (refs 10, 11). These two states can be distinguished in terms of their lattice distortion associated with the competition between strength of the itinerary denoted by resonance transfer energy between two orbitals (T_{reso}) and strong e–ph interaction (λ). If $T_{reso} \ll \lambda \ll \hbar\omega$, where $\hbar\omega$ is the phonon energy, then stable SC state will occur

without lattice distortion known as inverse adiabatic process. However the CDW state is associated with lattice distortion subjected to $\hbar\omega \ll T_{reso} \ll \lambda$ known as adiabatic process, which occurs at low temperature in prismatic coordination and at high temperature in octahedral coordination[7,12]. We have already reported the existence of CDW state at $T_{cdw} = 42$ K in 4H-NbSe$_2$ higher than $T_{cdw} = 35$ K in 2H-NbSe$_2$, irrespective of their stacking order as expected related to coordination.

Here, we propose an analytical expression for the correlation between T_{sc} and T_{cdw} at strong e–ph interaction accompanied with phonon energy in which stability of the CDW state is decided by the SC state and vice-versa. The analytical expression is verified using the pressure effect data of 2H-NbSe$_2$ (ref. 13).

The growth of single crystals 2H-NbSe$_2$ and 4H-NbSe$_2$ from polycrystalline compounds has been explained in our previous study[3]. From room-temperature powder X-ray diffraction, lattice constants were reported as $a \approx 3.445$ Å, $c \approx 2 \times 6.278$ Å in 2H-NbSe$_2$ and $a \approx 3.436$ Å, $c \approx 4 \times 6.298$ Å in 4H-NbSe$_2$.

The temperature-dependent resistivity of 2H- and 4H-NbSe$_2$ is shown in Figure 1 with room-temperature resistivity $\sim 11.4 \times 10^{-4}$ Ω-cm for 4H-NbSe$_2$, which is 16 times larger than 2H-NbSe$_2$, i.e. $\sim 6.8 \times 10^{-5}$ Ω-cm. This difference in resistivity is retained up to the lowest temperature of 60 K. Below 60 K, the difference in resistivity gradually increases till resistivity of individual compounds drops to zero. The large resistivity on 4H-NbSe$_2$ compared to 2H-NbSe$_2$ has already been explained using scattering time of free-electron model along with the co-existence of SC and CDW states, i.e. $T_{sc} = 7.4$ K, $T_{cdw} = 35$ K in 2H-NbSe$_2$, and $T_{sc} = 6.5$ K, $T_{cdw} = 42$ K in
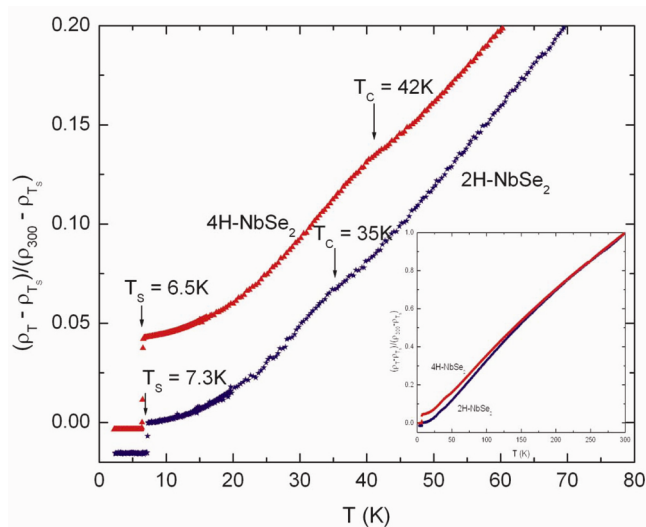

Figure 1. 2H- and 4H-NbSe$_2$ single crystals showing charge density wave and superconducting transition temperatures. (Inset) Normalized resitivity from 2 to 300 K.

*For correspondence. (e-mail: indrajit_naik@yahoo.co.in)

4H-NbSe$_2$ (ref. 3). According to the free-electron model, the resistivity in a normal metal is expressed as

$$\rho = \frac{m}{N(0)e^2\tau}. \tag{1}$$

Here symbols have their usual meaning. From the hexagonal lattice constants, the crystallographic parameters c/a are calculated as ~1.822 and 1.832 for 2H- and 4H-NbSe$_2$ respectively, which indicates that the normal density of states in 4H-NbSe$_2$ narrow d-band is large compared to 2H-NbSe$_2$. Therefore, in the present study we have given more emphasis on the density of states (DOS) associated with e–ph interaction (λ) and phonon energy ($\hbar\omega$) which affects T_{sc} and T_{cdw} in NbSe$_2$, irrespective of the unit cell size and stacking order therein.

There is controversy regarding theoretical formula for calculating the superconducting transition temperature T_{sc} in the strong e–ph interaction. Generally the formula for T_{sc} obtained by McMillan is widely used in the strong e–ph interaction limit[14]. However, Allen and Dynes[15] have proved from detailed numerical studies of Eliashberg equation that McMillan equation is not valid for large e–ph interaction. Therefore, Louie and Cohen derived an expression of T_{sc} for all ranges of e–ph interaction by solving analytically the Eliashberg equation in Matsubara representation using a model gap function[16]. In the weak e–ph interaction (λ_{sc}) limit it is expressed as

$$k_B T_{sc} = 1.13\hbar\sqrt{\langle\omega_{sc}^2\rangle}\exp\left\{-\frac{(1+\lambda_{sc})}{\lambda_{sc}}\right\}f(\beta). \tag{2}$$

Here $f(\beta)$ is the factor of order unity. This expression is similar to the familiar McMillan exponential form for small e–ph interaction when Coulomb interaction μ^* is neglected. If $1 \gg \lambda_{sc}$, then eq. (2) reduces to the Bardeen–Cooper–Schrieffer (BCS) formula. However, for the strong e–ph limit ($1 \ll \lambda_{sc}$), it becomes

$$k_B T_{sc} = 0.1824\hbar\sqrt{\lambda_{sc}\langle\omega_{sc}^2\rangle}. \tag{3}$$

This asymptotic form of T_{sc} is identical to that obtained numerically by Allen and Dynes[15] for very strong e–ph interaction.

According to Peierls' instability, the formation of CDW in one-dimensional system at $q = 2k_F$ defines the following relation[17]

$$k_B T_{cdw} = 1.14\varepsilon_F \exp\{-1/\lambda_{cdw}\}. \tag{4}$$

Here, λ_{cdw} is the dimensionless e–ph interaction and $\varepsilon_F = \hbar^2 k_F^2 / 2m$, which implies that $\hbar\omega_{cdw} = 2\varepsilon_F$ according to dispersion relation of acoustic phonon. Equation (4) is also quite similar to the BCS formula for SC transition temperature.

It can be clearly noticed from Figure 1 that increase in DOS in 4H-NbSe$_2$ increases T_{cdw} and decreases T_{sc} with respect to T_{cdw} and T_{sc} of 2H-NbSe$_2$ single crystal. In 4H-NbSe$_2$ the magnitude of change in T_{cdw}, i.e. ΔT_{cdw} is different from that in T_{sc}, i.e. ΔT_{sc}. A similar kind of change was also reported on 2H-NbSe$_2$ under pressure[13]. Here T_{cdw} and T_{sc} are changing in opposite directions; therefore, we have changed the sign of the exponent in the exponential function to positive in eq. (4). Again, both T_{cdw} and T_{sc} individually depend on DOS associated with e–ph interaction and phonon energy according to eqs (2)–(4). Therefore, in the present study, we obtain the relation between T_{cdw} and T_{sc} by assuming $\hbar\omega_{cdw} = \hbar\sqrt{\langle\omega_{sc}^2\rangle}$ and $\lambda_{cdw} = \lambda_{sc} = \lambda$.

If $\hbar\omega_{cdw} = \hbar\sqrt{\langle\omega_{sc}^2\rangle}$, then an analytical relation is derived from eqs (2) and (4) as follows

$$2T_{cdw} = \exp\left\{1 + \frac{1}{\lambda_{sc}} + \frac{1}{\lambda_{cdw}}\right\}T_{sc}. \tag{5}$$

Taking logarithm on both sides of the above equation, we get

$$\ln T_{cdw} = \left\{1 + \frac{1}{\lambda_{sc}} + \frac{1}{\lambda_{cdw}}\right\} + \ln\left(\frac{T_{sc}}{2}\right). \tag{6}$$

This analytical expression is equivalent to a straight-line expression, i.e. $y = mx + c$ having slope $m = 1$ and intercept constant $c = 1 + (1/\lambda_{sc}) + (1/\lambda_{cdw})$, which establishes a relation between T_{cdw} and T_{sc}. To verify eq. (6), we have fitted the pressure effect data of 2H-NbSe$_2$ in a ln–ln scale as shown in Figure 2, which provides $m \approx -2.25$ and $c \approx 6.37$. This contradicts the theoretical value of m; as a
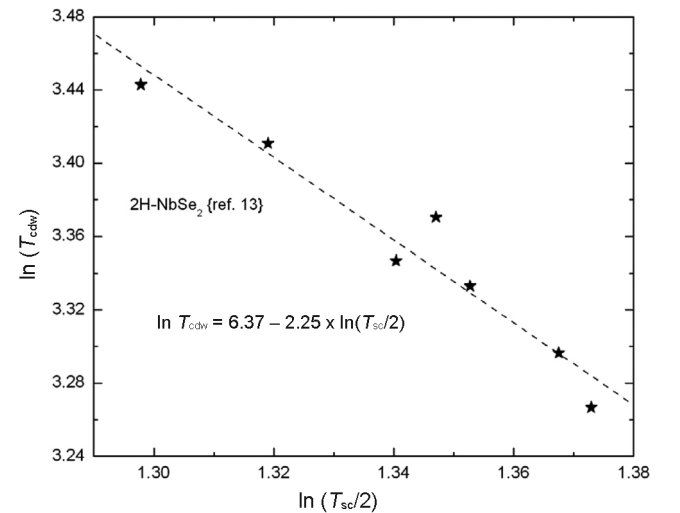

Figure 2. Pressure effect T_{cdw} and T_{sc} of 2H-NbSe$_2$ single crystal[13] fitted by $\ln T_{cdw} = c + m \times \ln(T_{sc}/2)$.
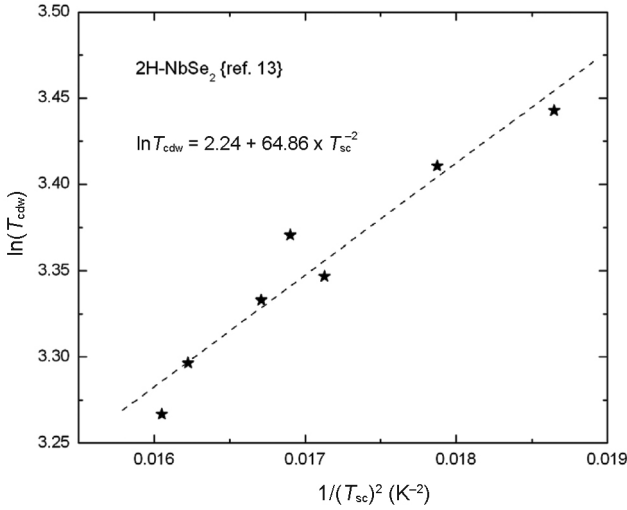
Figure 3. Pressure effect T_{cdw} and T_{sc} of 2H-NbSe$_2$ single crystal[13] fitted by $\ln T_{cdw} = c + (m/T_{sc}^2)$.

consequence, the possibility of $\hbar\omega_{cdw} = \hbar\sqrt{\langle\omega_{sc}^2\rangle}$ is rejected. This is also supported by experimental results in which 2H-NbSe$_2$ evolves with a new acoustic phonon energy accompanied by hardening below a static distortion at T_{cdw}, when the temperature decreases such that the phonon dispersions are similar at 8 and 50 K (refs 18–20). At 50 K, phonon energy ~3.7 meV has been reported near the wave vector $Q = (a/3, 0, 0)$.

If $\lambda_{cdw} = \lambda_{sc} = \lambda$, then an analytical relation is derived from eqs (3) and (4) as

$$k_B T_{cdw} = 1.14\varepsilon_F \exp\left\{\frac{(0.1824\hbar)^2\langle\omega_{sc}^2\rangle}{k_B^2 T_{sc}^2}\right\}. \quad (7)$$

Taking logarithm on both sides of the above equation, we get

$$\ln T_{cdw} = \ln\left(\frac{1.14\varepsilon_F}{k_B}\right) + \left\{\frac{(0.1824\hbar)^2\langle\omega_{sc}^2\rangle}{k_B^2 T_{sc}^2}\right\}. \quad (8)$$

This analytical expression is equivalent to a straight-line expression, i.e. $y = mx + c$ having slope $m \approx (0.1824\hbar)^2\langle\omega_{sc}^2\rangle$ and intercept constant $c = \ln(1.14\varepsilon_F/k_B)$, which establishes a relation between T_{cdw}, T_{sc}, $\hbar\omega_{cdw}$ and $\hbar\sqrt{\langle\omega_s^2\rangle}$. From the above expression, we can calculate any one quantity out of transition temperature and phonon energy of stable CDW state, if one quantity of CDW and all other quantities of SC are known and vice-versa. However, the reported pressure effect data on 2H-NbSe$_2$ are well fitted by the above analytical equation (eq. (8)) with best-fitting parameters $m \approx 64.86$ and $c \approx 2.24$ (Figure 3). Using $m \approx 64.86$ and $c \approx 2.24$ along with T_{sc} values in eq. (8) for 2H- and 4H-NbSe$_2$, we have determined $T_{cdw} \sim 31$ K for 2H-NbSe$_2$ and ~43 K for 4H-NbSe$_2$, close to their

experimental values. We have also calculated phonon energies $\hbar\sqrt{\langle\omega_{sc}^2\rangle} \approx 3.8$ meV and $\hbar\omega_{cdw} \approx 1.4$ meV from $m \approx 64.86$ and $c \approx 2.24$ for SC and CDW states respectively. Though, our calculated value of $\hbar\omega_{cdw}$ is less compared to the reported results of Ayache et al.[18] the $\hbar\sqrt{\langle\omega_{sc}^2\rangle}$ is found very close to the phonon energy at 50 K (refs 18–20). Besides this discrepancy in $\hbar\omega_{cdw}$, eq. (8) provides best results for both 2H- and 4H-NbSe$_2$.

In this study, we have made an attempt to correlate the SC and CDW states on NbSe$_2$ through constant phonon energy, i.e. $\hbar\omega_{cdw} = \hbar\sqrt{\langle\omega_{sc}^2\rangle}$ and constant e–ph interaction, i.e. $\lambda_{cdw} = \lambda_{sc} = \lambda$. The constant phonon energy condition violates the experimental results; as a consequence, we reject the analytical expression. However, the analytical expression derived from constant e–ph interaction, i.e. $\lambda_{cdw} = \lambda_{sc} = \lambda$ condition explains the change in T_{cdw} and T_{sc}, both qualitatively and quantitatively on 2H- and 4H-NbSe$_2$. It also provides the phonon energies $\hbar\sqrt{\langle\omega_{sc}^2\rangle} \approx 3.8$ meV and $\hbar\omega_{cdw} \approx 1.4$ meV for SC and CDW states respectively, from its best-fitting parameters, i.e. $m \approx 64.86$ and $c \approx 2.24$. Therefore, we claim that the SC and CDW transitions in NbSe$_2$ are affected significantly by DOS associated with constant e–ph interaction and are related with each other according to the analytical equation, i.e. eq. (8).

1. Kadijk, F. and Jellinek, F., On the polymorphism of niobium diselenide. *J. Less Common Met.*, 1971, **23**, 437–441.
2. Naito, M. and Tanaka, S., Electrical transport properties in 2H-NbS$_2$, -NbSe$_2$, -TaS$_2$ and –TaSe$_2$. *J. Phys. Soc. Jpn.*, 1982, **51**, 219–227.
3. Naik, I. and Rastogi, A. K., Charge density wave and superconductivity in 2H- and 4H-NbSe$_2$: a revisit. *Pramana – J. Phys.*, 2011, **76**(6), 957–963.
4. Doran, N. J., Ricco, B., Schreiber, M., Titterington, D. and Wexler, G., The electronic susceptibility and charge density waves in 2H-NbSe$_2$ layered compound. *J. Phys. C*, 1978, **11**, 699–705.
5. Rice, T. M. and Scott, G. K., New mechanism for a charge density wave instability. *Phys. Rev. Lett.*, 1975, **35**, 120–123.
6. Moncton, D. E., Axe, J. D. and Disalvo, F. J., Neutron scattering study of the charge density wave transitions in 2H-TaSe$_2$ and 2H-NbSe$_2$. *Phys. Rev. B*, 1977, **16**, 801–819.
7. Giambattista, B., Johnson, A., Coleman, R. V., Drake, B. and Hansma, P. K., Charge density wave observed at 4.2 K by scanning-tunneling microscopy. *Phys. Rev. B*, 1988, **37**, 2741–2744.
8. Berthier, C., Jerome, D. and Molinie, P., NMR study on a 2H-NbSe$_2$ single crystal: A microscopic investigation of the charge density wave states. *J. Phys. C*, 1978, **11**, 797–814.
9. Du, C-H. et al., X-ray scattering studies of 2H-NbSe$_2$, a superconductor and charge density wave material, under high external magnetic fields. *J. Phys.: Condens. Matter*, 2000, **12**, 5361–5370.
10. Li, L., Xu, Z., Shen, J., Qiu, L. and Gan, Z., Effect of charge density wave transition on the transport properties of 2H-NbSe$_2$. *J. Phys.: Condens. Matter*, 2005, **17**, 493–498.
11. Naik, I. and Rastogi, A. K., Transport properties of 2H-NbSe$_2$: effect of Ga-intercalation. *Physica B*, 2010, **405**, 955–957.
12. Thompson, A. H., Pauling's ionicity and charge density wave in layered transition metal dichalcogenides. *Phys. Rev. Lett.*, 1975, **34**, 520–524.
13. Chu, C. W., Diatschenko, V., Huang, C. Y. and Disalvo, F. J., Pressure effect on the charge density wave formation on 2H-NbSe$_2$

and correlation between structural instabilities and superconductivity in unstable solids. *Phys. Rev. B*, 1977, **15**, 1340–1342.

14. McMillan, W. L., Transition temperatures of strong-coupled superconductors. *Phys. Rev.*, 1968, **167**, 331–344.
15. Allen, P. B. and Dynes, R. C., Transition temperature of strong-coupled superconductors reanalyzed. *Phys. Rev. B*, 1975, **12**, 905–922.
16. Louie, S. G. and Cohen, M. L., Superconducting transition temperatures for weak and strong electron–phonon coupling. *Solid State Commun.*, 1977, **22**, 1–4.
17. Berlinsky, A. J., One-dimensional metals and charge density wave effects in these materials. *Rep. Prog. Phys.*, 1979, **42**, 1243–1283.
18. Ayache, C., Currat, R. and Molinie, P., Study of the mode softening in $NbSe_2$-2H. *Physica B*, 1992, **180–181**, 333–335.
19. Weber, F. *et al.*, Extended phonon collapse and the origin of the charge density wave in $2H-NbSe_2$. *Phys. Rev. Lett.*, 2011, **107**, 107403-(1-5).
20. Schmalzl, K., Strauch, D., Hiess, A. and Berger, H., Temperature dependent phonon dispersion in $2H-NbSe_2$ investigated using inelastic neutron scattering. *J. Phys.: Condens. Matter*, 2008, **20**, 104240-(1-3).

Selecting clinical and laboratory methods of manufacture of orthopaedic titanium alloy structures using a biopotentiometer

Alexei V. Yumashev*, Anatolij S. Utyuzh, Maria V. Mikhailova, Vadim O. Samusenkov and Ilona R. Volchkova

Department of Orthopedic Dentistry,
I. M. Sechenov First Moscow State Medical University,
Moscow 119991, Russia

The present communication aims at determining an optimum method of manufacture of orthopaedic arch titanium alloy dentures that would not cause galvanosis in patients using such dentures. A clinical randomized controlled retrospective study was conducted. Sixty patients who used arch titanium alloy dentures were examined. Three measurements of electrochemical potentials in various areas of the oral cavity were done in all patients, using a biopotentiometer. Linear prediction of differences in potentials in measurement areas 1–3 for the control group (CG) of patients exhibited minor growth dynamics, which can be indicative of the risk of galvanosis in CG patients in the future.

Keywords: Biopotentiometry, dentistry, dentures, galvanosis, galvanic currents, titanium alloys.

*For correspondence. (e-mail: yumashev031996@mail.ru)

ONE of the problems in patients using metal dentures is the emergence of galvanic currents leading to galvanosis. This depends greatly on the correct choice of clinical and laboratory methods of denture manufacture. Despite the fact that removable dentures are still available in dental practice, fixed dentures have lately been in demand among patients[1,2].

Intolerance to dentures made of metal alloys in the oral cavity is a pressing problem in dentistry. It was reported that the use of fixed metal dentures may cause various dental pathologies[3–6]. However, there is no alternative to metal dentures for now, because of low physical and chemical properties of other materials, which includes high-breaking frequency[7,8]. Combination of metals and other materials, for example, ceramics, zirconium dioxide and others, is considered the most acceptable alternative option[9–13]. Nevertheless, the use of additional materials, in combination with metals, does not solve the problem of such metal structures in the mouth which affect biomedical parameters of patients[14–17].

Another important requirement to fixed structures in oral cavity is high wear resistance and minimum adverse effects[17]. Titanium and titanium alloys are among materials that are widely used in dentistry for making metal dentures. Titanium alloys are usually manufactured by milling and casting[18]. Sophisticated dental treatment methods are becoming increasingly common place, including those that use titanium alloys. Such alloys are cast in a furnace at high temperatures and milled via CAD/CAM technology[19]. The alloys differ drastically by the type of their surface, which is well seen on micrographs (Figure 1).

At the moment, titanium alloys of all types from different manufacturing techniques are used equally. At the same time, the question of preference still remains. The fact that no preference has been given to any manufacturing technique of titanium alloy is explained by the fact that titanium itself is one of the most bio-friendly materials that satisfies the physical and chemical requirements of dentures[20,21].

In the case of using a titanium alloy, the impossibility of using recoverable materials is also the undoubted advantage of its processing, as this feedback differs significantly from the original materials in composition and properties, thus leading to a decrease in the quality of orthopaedic structures: cast surface defects, intensive